Universität des Saarlandes

Fachrichtung 6.1 – Mathematik

Preprint Nr. 362

An iterative method for EIT involving only solutions of Poisson equations. I: Mesh-free forward solver

Thorsten Hohage and Sergej Rjasanow

Saarbrücken 2015

Fachrichtung 6.1 – Mathematik
Universität des Saarlandes

Preprint No. 362
submitted: June 26, 2015

An iterative method for EIT involving only solutions of Poisson equations. I: Mesh-free forward solver

Thorsten Hohage

Georg-August-Universitt Göttingen
Institut für Numerische und Angewandte Mathematik
Lotzestr. 16-18
37083 Göttingen
Deutschland
adal@domain.de

Sergej Rjasanow

Universität des Saarlandes
Fachrichtung Mathematik
Postfach 15 11 50
66041 Saarbrücken
Deutschland
bebe@domain.de

Edited by
FR 6.1 – Mathematik
Universität des Saarlandes
Postfach 15 11 50
66041 Saarbrücken
Germany

Fax: + 49 681 302 4443
e-Mail: preprint@math.uni-sb.de
WWW: http://www.math.uni-sb.de/

An iterative method for EIT involving only solutions of Poisson equations. I: Mesh-free forward solver

Thorsten Hohage & Sergej Rjasanow

June 26, 2015

Abstract

An iterative procedure for the numerical solution of both the forward and the inverse problem of Electrical Impedance Tomography (EIT) is formulated. As opposed to existing iterative regularisation methods such as nonlinear Landweber iteration or Newton-type methods it does not require the solution of multiple forward problems. In fact, no meshing of the domain is required. In each iteration step updates of the electric potential and the conductivity are computed by solving simple Poisson equations. For the repeated solution of the Poisson equation we suggest a combination of the Boundary Element Method (BEM) and Radial Basis Functions (RBF).

In this paper we consider the case that the update of the conductivity is omitted, which yields an iterative method for the forward problem. We prove linear convergence with a convergence factor depending on the ratio of the maximal and the minimal value of the conductivity. We use a fast version of the Boundary Element Method based on the Adaptive Cross Approximation (ACA) for the approximation of dense matrices. Numerical examples illustrate the functionality and the efficiency of the approach.

1 Introduction

Electrical Impedance Tomography consists in reconstructing the electric conductivity of a body from boundary measurements of voltages and currents. It is a classical inverse problem with applications in medical imaging and nondestructive testing (see e.g. the reviews [3, 11] and numerous references therein). The same mathematical model also describes other stationary diffusion processes, e.g. in heat conduction.

It is beyond the scope of this paper to completely review numerical methods for EIT, we refer the reader to the reviews cited above. One popular class of numerical methods consists in formulating the problem as a nonlinear operator equation and applying iterative regularisation methods such as Landweber iteration, the Newton-CG, the Levenberg-Marquardt, or the Iteratively Regularised Gauss-Newton method (see [5] for an overview).

All of these methods involve repeated costly evaluations of the forward operator.

Another class of reconstruction methods implement uniqueness proofs based on geometrical optics solutions (see e.g. [10, 6]). They exhibit global convergence, but are conceptually fairly complicated and also nontrivial to implement. Moreover, they are much less flexible concerning modifications of the problem setup than iterative regularisation methods.

The method suggested in this paper has the advantage of being comparatively simple to implement: Essentially it involves only the solution of Poisson equations. Of course, the Poisson equations (as well as the full forward problem) can be solved efficiently by the finite element method, and we have implemented both to get numerical reference solutions for our tests.

As an alternative, we suggest to solve the Poisson equations by using special RBF's to reconstruct particular solutions of the Poisson equation violating the boundary condition (see [1]) combined with a fast BEM (see [8]) to correct the boundary condition by solving a Laplace equation. If the domain is a ball, the BEM may be replaced by an implementation of the Poisson formula.

If the update of the conductivity is omitted our method yields an iterative method for the solution of the forward problem. Even though it is not competitive compared to high order finite elements we believe it is of some interest due to its simplicity. We prove linear convergence of the iteration scheme with optimal convergence factor $\frac{\alpha_{\max}-\alpha_{\min}}{\alpha_{\max}+\alpha_{\min}}$ where $\alpha_{\max}$ and $\alpha_{\min}$ are the maximal and minimal values of the conductivity.

The paper is organised as follows. A model problem of the three-dimensional heat conduction equation is formulated in Section 2. In Section 3, we formulate a new iterative algorithm for the solution of the forward problem and prove its convergence. A FEM solution of the problem is described in Section 4 and the BEM solution in Section 5. A series of numerical examples for both the FEM and the BEM approach as well as for the RBF interpolation are presented in the final Section 6.

2 Formulation of the problem

In this paper, we consider the following boundary value problem

$$
\begin{aligned}
-\operatorname{div}\alpha(x)\ \operatorname{grad} u(x) &= 0\,, \quad \text{for } x\in\Omega\,, && \text{(1a)}\\
\gamma_0 u(x) &= 0\,, \quad \text{for } x\in\Gamma_0\,, && \text{(1b)}\\
\gamma_0 u(x) &= u_1(x)\,, \quad \text{for } x\in\Gamma_1\,, && \text{(1c)}
\end{aligned}
$$

where

$$\alpha\in L_\infty(\overline{\Omega})\,,\ 0<\alpha_{\min}\le\alpha(x)\le\alpha_{\max}$$

is the conductivity. The boundary of the three-dimensional simply connected Lipschitz domain $\Omega\in\mathbb{R}^3$ consists of two parts Γ_0 and Γ_1 fulfilling

$$\overline{\Gamma}_0\cup\overline{\Gamma}_1=\Gamma=\partial\Omega\,.$$

Our main example later on will be the unit cube and its upper face will be the Γ_1 part of the boundary

$$\Omega = (0,1)^3\,, \quad \Gamma = \partial\Omega\,, \quad \Gamma_1 = \left\{x \in \Gamma \,:\, x_3 = 1\right\}.$$

The operator

$$\gamma_0 \,:\, H^1(\Omega) \to H^{1/2}(\Gamma)$$

is the usual Dirichlet trace operator and $u_1 \in H^{1/2}(\Gamma_1)$ is the given non-trivial boundary condition. Under these assumptions, the direct boundary value problem has a unique weak solution $u \in H^1(\Omega)$.

The inverse problem is formulated as follows. On the part of the boundary Γ_1 a signal u_1 is applied and the interior conormal derivative of the resulting solution u

$$\gamma_1 u(x) = \lim_{\tilde{x}\to x} (\operatorname{grad}_{\tilde{x}} u(\tilde{x}), n_x)\,,\ x \in \Gamma_1\,,\ \tilde{x} \in \Omega \tag{2}$$

is measured. In (2), n_x denotes the outer normal vector at x which is defined for almost all $x \in \Gamma_1$. From this additional information, we will try to estimate the material parameter $\alpha(x)$ for all $x \in \Omega$. In addition, we assume that a typical value α^* for the material parameter α is known. There are two possible situations, either the variable material parameter α differs only slightly from its typical value α^* or the part of the domain Ω where the difference is there is rather small.

3 An iterative method for the solution of the forward problem

3.1 Derivation of the iteration formula for the forward problem

By the use of a typical value α^*, we rewrite the equation (1) as follows

$$-\Delta u(x) = \operatorname{div}\left(\frac{\alpha(x)}{\alpha^*} - 1\right) \operatorname{grad} u(x)\,, \quad x \in \Omega\,. \tag{3}$$

The idea is now to formulate an iterative process for an approximative solution of the problem (3). Starting from

$$u_0(x) = 0\,, \quad x \in \Omega\,,$$

we iterate

$$\begin{aligned} &\text{For } k = 0, 1, \ldots \\ &\quad \text{Solve } \begin{cases} -\Delta u_{k+1} = \operatorname{div}\left(\dfrac{\alpha}{\alpha^*} - 1\right) \operatorname{grad}\, u_k & \text{in } \Omega \\ \gamma_0 u_{k+1} = (0, u_1) & \text{on } \Gamma_0 \cup \Gamma_1. \end{cases} \end{aligned} \tag{4}$$

Thus, the iterative process consists in a numerical solution of the Laplace equation in the initial step and a sequence of the Poisson problems during the iteration. Problems of this type can be solved efficiently by the FEM or by the use of the fast BEM as discussed in Sections 4 and 5.

3.2 Convergence analysis

We define the norm on $H_0^1(\Omega)$ by

$$\|u\|_{H_0^1} := \left(\int_\Omega |\operatorname{grad} u|^2 \, dx \right)^{1/2}.$$

Recall that due to the Poincaré-Friedrich inequality $\|u\|_{L^2} \le c\|\operatorname{grad} u\|_{L^2}$ for $u \in H_0^1(\Omega)$ the norm $\|\cdot\|_{H_0^1}$ is equivalent to the norm $\|u\|_{H^1} := (\int_\Omega |u|^2 + |\operatorname{grad} u|^2 \, dx)^{1/2}$.

Theorem 1. *Let u denote the solution to (1), and let u_k be defined by (4).*

1. *The iterates u_k satisfy the error estimate*

$$\|u_k - u\|_{H_0^1} \le \Theta^k \|u_0 - u\|_{H_0^1} \tag{5}$$

with the convergence factor

$$\Theta := \max\left(\frac{\alpha_{\max}}{\alpha^*} - 1, 1 - \frac{\alpha_{\min}}{\alpha^*} \right).$$

2. *Θ is minimal for the choice*

$$\alpha^* = \frac{\alpha_{\min} + \alpha_{\max}}{2},$$

and in this case

$$\|u_k - u\|_{H_0^1} \le \left(\frac{\alpha_{\max} - \alpha_{\min}}{\alpha_{\max} + \alpha_{\min}} \right)^k \|u_0 - u\|_{H_0^1}. \tag{6}$$

3. *The error bound (5) is optimal in the sense that for any $\tilde{\Theta} \in (0, \Theta)$ there exists a starting point u_0 such that*

$$\lim_{k\to\infty} \tilde{\Theta}^{-k} \|u_k - u\|_{H_0^1} = \infty.$$

In particular, the iteration diverges in general if $\alpha_{\max} > 2\alpha^*$.

Proof. 1. Let $u_* \in H^1(\Omega)$ be any function satisfying $\gamma_0 u_* = (0, u_1)$ and define

$$\beta = 1 - \frac{\alpha}{\alpha^*}.$$

Then $\tilde{u}_k = u_k - u_*$ belongs to $H_0^1(\Omega)$. It satisfies the variational equation

$$\langle \operatorname{grad} \tilde{u}_{k+1}, \operatorname{grad} v \rangle_{L_2} = \langle \beta \operatorname{grad} \tilde{u}_k, \operatorname{grad} v \rangle_{L_2} + \langle (\beta - 1) \operatorname{grad} u_*, \operatorname{grad} v \rangle_{L_2} \tag{7}$$

for all $v \in H_0^1(\Omega)$. For $\tilde{\beta} \in L^\infty(\Omega)$ let $L_{\tilde{\beta}} : H_0^1(\Omega) \to H_0^1(\Omega)' = H^{-1}(\Omega)$ denote the operator defined implicitly by

$$\left\langle L_{\tilde{\beta}} u, v \right\rangle_{H^{-1}, H_0^1} = \left\langle \tilde{\beta} \operatorname{grad} u, \operatorname{grad} v \right\rangle_{L_2}, \qquad u, v \in H_0^1(\Omega).$$

Note that $L_{\tilde\beta}$ is bounded with $\|L_\beta\|_{L(H_0^1(\Omega),H^{-1}(\Omega))}\| \le \|\tilde\beta\|_\infty$. Moreover, define $U_* \in H^{-1}(\Omega)$ by $U_*(v) := \langle(\beta-1)\operatorname{grad} u_*, \operatorname{grad} v\rangle_{L^2}$. Then we can write

$$\tilde u_{k+1} = L_1^{-1}L_\beta \tilde u_k + L_1^{-1}U_*.$$

By the definition of the dual norm L_1 is isometric, so

$$\|L_1^{-1}L_\beta\|_{L(H_0^1(\Omega))} \le \|L_1^{-1}\|_{L(H_0^1(\Omega),H^{-1}(\Omega))}\,\|L_\beta\|_{L(H^{-1}(\Omega),H_0^1(\Omega))} \le \|\beta\|_\infty.$$

As

$$\|\beta\|_\infty = \frac{1}{\alpha^*}\|\alpha_{\max}-\alpha^*\|_\infty = \Theta, \tag{8}$$

this means that $u \mapsto L_1^{-1}L_\beta u + L_1^{-1}U_*$ is a contraction in $H_0^1(\Omega)$ with contraction number Θ if $\Theta < 1$. In this case we obtain by Banach's fixed point theorem that sequence $(\tilde u_k)$ converges to the unique fixed point $\overline{u}$ of (7) and $\|\tilde u_k - \overline{u}\| \le \Theta^k\|\tilde u_0 - \overline{u}\|$. ¿From the derivation we see that $\overline{u} = u - u_*$. This implies the first assertion for the case $\Theta < 1$. Alternatively, we could have derived the result directly from the identity

$$\tilde u_{k+1} - \overline{u} = L_1^{-1}L_\beta(\tilde u_k - \overline{u}) \tag{9}$$

by induction, which allows to treat the case $\Theta \ge 1$.
2. The second statement is an obvious consequence of the first statement.
3. Let $\tilde\Theta \in (0,\Theta)$. Recall that $\|\beta\|_\infty = \inf\{t \ge 0 : |\beta| \le t \text{ a.e. on } \Omega\}$. Due to (8) there exist a Lebesgue-measurable set $A \subset \Omega$ with positive Lebesgue measure such that

$$|\beta(x)| \ge \frac{1}{2}(\tilde\Theta + \Theta) \qquad \text{for all } x \in A.$$

Let us introduce the seminorm

$$|w|_A := \Big(\int_A |\operatorname{grad} w|^2\,dx\Big)^{1/2}$$

on $H_0^1(\Omega)$ and the corresponding bilinear form

$$\langle w, v\rangle_A := \int_A (\operatorname{grad} w, \operatorname{grad} v)\,dx\,.$$

For $w \in H_0^1(\Omega)$ with $|w|_A > 0$, we have

$$\begin{aligned}|L_1^{-1}L_\beta w|_A &= \sup_{|f|_A\le 1}\big\langle L_1^{-1}L_\beta w, f\big\rangle_A = \sup_{|f|_A\le 1}\langle\beta\operatorname{grad} w, \operatorname{grad} f\rangle_A \\ &\ge \frac{1}{|w|_A}\langle\beta\operatorname{grad} w, \operatorname{grad} w\rangle_A \ge \frac{1}{2}(\tilde\Theta+\Theta)|w|_A\end{aligned}$$

where we have chosen $f := w/|w|_A$. Now choose u_0 such that $|\tilde u_0 - \overline{u}|_A > 0$. Then it follows from (9) that

$$|\tilde u_k - \overline{u}|_A \ge \left(\frac{\tilde\Theta+\Theta}{2}\right)^k |\tilde u_0 - \overline{u}|_A.$$

As $\|u_k - u\|_{H_0^1} \ge |\tilde u_k - \overline{u}|_A$, this implies the assertion. □

4 A FE method for the forward problem

In this section, we describe a simple finite element method for the direct problem (1). Let the domain Ω be a cuboid

$$\Omega = (0, L_1) \times (0, L_2) \times (0, L_3)$$

and its discretisation $\mathcal{K}_h$ consists of

$$N_E = N_1 \cdot N_2 \cdot N_3$$

identical hexahedral finite elements K of the size

$$h_1 = L_1/N_1\,,\ h_2 = L_2/N_2\,,\ h_3 = L_3/N_3\,.$$

The parameterisation of the element K is as follows

$$K = \left\{ x \in \Omega\ :\ x = x_c + \frac{1}{2} H\,\xi\,,\ \xi \in (-1,1)^3 \right\},$$

where $x_c \in K$ is the central point of the element K and

$$H = \mathrm{diag}(h_1, h_2, h_3) \in \mathbb{R}^{3\times 3}\,.$$

Let $\mathcal{N}_h = \mathcal{N}_{h,\Omega} \cup \mathcal{N}_{h,\Gamma}$ be the set of all nodes of the discretisation $\mathcal{K}_h$, where the number of the interior nodes

$$N = \#\mathcal{N}_{h,\Omega} = (N_1 - 1) \cdot (N_2 - 1) \cdot (N_3 - 1)$$

will be the number of degrees of freedom for the Dirichlet problem we consider here. Next, we introduce nodal trial functions φ_z for all $z \in \mathcal{N}_{h,\Omega}$ with $\varphi_z(z) = 1$, which are trilinear within eight finite elements which contain the node z and which are equal to zero on the outer boundaries of these eight elements. Thus, within each element K eight trial functions have non-zero values. On the reference element $(-1,1)^3$, the corresponding basis functions are defined as follows

$$\psi_\sigma(\xi) = \frac{1}{8}(1+\sigma_1\xi_1)(1+\sigma_2\xi_2)(1+\sigma_3\xi_3)\,,\ \xi = (\xi_1,\xi_2,\xi_3)^\top \in (-1,1)^3$$

and $\sigma = (\sigma_1, \sigma_2, \sigma_3)^\top$ is one of the eight nodes of the reference element $(-1,1)^3$, i.e. σ is of the form

$$\sigma = (\pm 1, \pm 1, \pm 1)^\top\,.$$

Thus within an element K, the trial function ψ_z is defined as

$$\varphi_z(x) = \psi_\sigma(\xi)\,,\ \xi = 2\,H^{-1}(x - x_c)\,.$$

The solution u of the Dirichlet problem

$$
\begin{aligned}
-\operatorname{div}\alpha(x)\ \operatorname{grad}\ u(x) &= f(x)\,, \quad \text{for } x \in \Omega\,, && \text{(10a)}\\
\gamma_0 u(x) &= g(x)\,, \quad \text{for } x \in \Gamma\,, && \text{(10b)}
\end{aligned}
$$

will be decomposed in a sum $u = u_0 + u_D$, where u_D is an extension of the Dirichlet datum g in Ω and u_0 fulfils the homogeneous Dirichlet boundary condition $\gamma_0 u_0(x) = 0\,,$ for $x \in \Gamma$. The weak formulation of the problem (10) reads: Find $u_0 \in H_0^1(\Omega)$ such that

$$
a_\Omega(u_0, v) = (f, v) - a_\Omega(u_D, v) \quad \text{for all } v \in H_0^1(\Omega)\,.
$$

The bilinear form a_Ω is

$$
a_\Omega(u, v) = \int_\Omega \alpha(x)\,(\operatorname{grad}\ u(x), \operatorname{grad}\ v(x))dx\,.
$$

Let

$$
V_h = \operatorname{span}(\varphi_z\,,\ z \in \Omega) \subset H_0^1(\Omega)
$$

be the ansatz space with $\dim V_h = N$. Then the discrete weak formulation of the problem (10) reads: Find $u_{0h} \in V_h$ such that

$$
a_\Omega(u_{0h}, v) = (f, v) - a_\Omega(u_{Dh}, v) \quad \text{for all } v \in V_h\,.
$$

This formulation is equivalent to a system of linear equations

$$
Ay = b\,,\ A \in \mathbb{R}^{N\times N}\,,\ y, b \in \mathbb{R}^N\,.
$$

The matrix of this system is symmetric and positive definite. Thus, the system can be solved with Conjugate Gradient Method (CGM). The entries of the matrix as well of the right hand side b can be computed with the help of the Gauss-quadrature on the reference element $(-1, 1)^3$. For an efficient practical realisation of this procedure it is necessary to find a simple and effective method for the extension of the Dirichlet boundary condition g to a function $u_{Dh} : \overline{\Omega} \to \mathbb{R}$. The most natural procedure is the interpolation on the boundary Γ

$$
u_{Dh} \in \operatorname{span}(\varphi_z\,,\ z \in \Gamma)\,,\ u_{Dh}(z) = g(z) \quad \text{for } z \in \Gamma\,.
$$

No numerical work is necessary to realise this interpolation.

5 A BE method for the forward problem

5.1 Boundary integral formulation

Boundary element methods can efficiently be applied to partial differential equations with constant coefficients. One of the most simple examples is the Dirichlet problem for the Poisson equation

$$
-\Delta u(x) = f(x) \quad \text{for } x \in \Omega\,, \quad \gamma_0 u(x) = g(x) \quad \text{for } x \in \Gamma\,. \qquad \text{(11)}
$$

The solution of this problem is given by the representation formula

$$u(x) = \int_\Gamma u^*(x,y)t(y)ds_y - \int_\Gamma \gamma_{1,y}u^*(x,y)g(y)ds_y + \int_\Omega u^*(x,y)f(y)dy \tag{12}$$

for $x \in \Omega$, where $t = \gamma_1 u$ is the unknown Neumann datum. The fundamental solution u^* of the Laplace equation is

$$u^*(x,y) = \frac{1}{4\pi}\frac{1}{|x-y|} \quad \text{for } x, y \in \mathbb{R}^3\,. \tag{13}$$

By applying the interior trace operator γ_0 to the representation formula (12) and using the jump relations (see e.g. [7]) and the Dirichlet boundary condition, we obtain the boundary integral equation

$$\int_\Gamma u^*(x,y)t(y)ds_y = \frac{1}{2}g(x) + \int_\Gamma \gamma_{1,y}u^*(x,y)g(y)ds_y - \int_\Omega u^*(x,y)f(y)dy \tag{14}$$

for $x \in \Gamma$. Thus, we have to solve a first kind boundary integral equation to find $t \in H^{-1/2}(\Gamma)$ such that

$$(Vt)(x) = \frac{1}{2}g(x) + (Kg)(x) - (Nf)(x) \quad \text{for } x \in \Gamma\,, \tag{15}$$

where V denotes the single layer, K the double layer and N the Newton potential.

5.2 Particular solution

The drawback in considering the boundary integral equation (15) is the evaluation of the Newton potential Nf. Besides a direct computation, there exist several approaches leading to more efficient methods. One of the most effective is the particular solution approach. Let u_p be a particular solution of Poisson equation in (11) satisfying

$$-\Delta u_p(x) = f(x) \quad \text{for } x \in \Omega\,.$$

Then, instead of (11), we consider a Dirichlet boundary value problem for the Laplace operator,

$$-\Delta u_h(x) = 0 \quad \text{for } x \in \Omega, \quad \gamma_0 u_h(x) = g(x) - \gamma_0 u_p(x) \quad \text{for } x \in \Gamma\,.$$

The solution u of (11) is then given by $u_h + u_p$. The unknown Neumann datum $t_h = \gamma_1 u_0$ is the unique solution of the boundary integral equation

$$(Vt_h)(x) = \frac{1}{2}\left(g(x) - \gamma_0 u_p(x)\right) + \left(K\big(g - \gamma_0 u_p\big)\right)(x) \quad \text{for } x \in \Gamma\,.$$

This equation is equivalent to the variational problem

$$\Big\langle Vt_h, w\Big\rangle_\Gamma = \Big\langle \Big(\frac{1}{2}I + K\Big)\tilde{g}, w\Big\rangle_\Gamma \quad \text{for all } w \in H^{-1/2}(\Gamma),$$

where $\tilde{g} = g - \gamma_0 u_p$ is the modified boundary condition. Often, the right hand side f is not given analytically but, as a rule, is the result of a numerical procedure. In this case it is impossible, however, also not necessary to find the exact particular solution of the inhomogeneous problem. The idea is to approximate the right hand side in such a way that an approximate particular solution can be found and used instead of the exact.

Let $\{\phi_1, \ldots, \phi_{N_p}\}$ be a system of functions having the property that each of the Poisson equations

$$-\Delta\psi_j(x) = \phi_j(x)\,, \quad j = 1, \ldots, N_p \tag{16}$$

has a known analytical solution ψ_j. Then an approximation of the right hand side f of the form

$$f_{N_p}(x) = \sum_{j=1}^{N_p} f_j \phi_j(x) \tag{17}$$

provides an approximate particular solution

$$u_{N_p}(x) = \sum_{j=1}^{N_p} f_j \psi_j(x)\,. \tag{18}$$

The approximation (17) can be found either by the interpolation in a set of N_p points

$$f(x_i) = f_{N_p}(x_i) = \sum_{j=1}^{N_p} f_j \phi_j(x_i)\,, \quad i = 1, \ldots, N_p\,. \tag{19}$$

For compactly supported functions ϕ_j, the L_2-projection is also possible

$$\Big\langle f, \phi_i\Big\rangle_{L_2} = \Big\langle f_{N_p}, \phi_i\Big\rangle_{L_2} = \sum_{j=1}^{N_p} f_j \Big\langle \phi_j, \phi_i\Big\rangle_{L_2}\,, \quad i = 1, \ldots, N_p\,. \tag{20}$$

In both cases a system of linear equations has to be solved. For the special form of the right hand side given in (3), the interpolation method (19) is probably less convenient since it poses high requirements on the smoothness of the functions α and u_k. However, the L_2-projection seems to be perfect

$$\Big\langle f, \phi_i\Big\rangle_\Omega = \int_\Omega \operatorname{div}\Big(\Big(\frac{\alpha(x)}{\alpha^*} - 1\Big)\ \operatorname{grad}\ u_k(x)\Big)\phi_i(x)\,dx = \tag{21}$$

$$= -\int_\Omega \Big(\frac{\alpha(x)}{\alpha^*} - 1\Big)\ (\operatorname{grad}\ u_k(x), \operatorname{grad}\phi_i(x))\,dx + \tag{22}$$

$$+ \int_\Gamma \Big(\frac{\alpha(x)}{\alpha^*} - 1\Big)\,\gamma_1 u_k(x)\phi_i(x)\,ds_x\,. \tag{23}$$

While the conormal derivative $\gamma_1 u_k$ is known as a direct result of the BEM procedure, the gradient grad u_k inside the domain Ω has to be computed via the representation formula (12).

5.3 Radial basis functions

Radial basis functions are one of the most popular tools for interpolating or approximating scattered data in various applications. A single radial basis function $\phi : \mathbb{R}^3 \to \mathbb{R}$ is a real-valued function whose value depends only on the distance from the origin, i.e.

$$\phi(x) = \phi(|x|) \quad \text{for } x \in \mathbb{R}^3 .$$

Given a set of distinct points

$$\left\{x_1, \ldots, x_{N_p}\right\} \subset \overline{\Omega} ,$$

a system $\left\{\phi_1, \ldots, \phi_{N_p}\right\}$ can be defined as follows

$$\phi_j(x) = \phi(|x - x_j|) , \quad j = 1, \ldots, N_p . \tag{24}$$

In the following we describe the use of radial basis functions to construct special solutions to the Poisson equation (see [9, 4]).

The first two columns of Table 1 list some popular radial basis functions. The Wendland functions $\phi_{3,k}$ are compactly supported in the unit ball and belong to the space C^{2k}. In practice a scaling parameter $\beta > 0$ should be introduced, i.e. $\phi(\rho)$ should be replaced by $\phi(\rho/\beta)$.

Since the functions ϕ are isotropic, we get in spherical coordinates instead of the Poisson equation an ordinary differential equation

$$\psi''(\varrho) + \frac{2}{\varrho}\psi'(\varrho) = -\phi(\varrho) . \tag{25}$$

To avoid singularities at zero, we complete the equation (25) with the initial conditions

$$\psi(0) = \psi_0 , \quad \psi'(0) = 0.$$

If a scaled version $\phi(\rho/\beta)$ of the radial basis function with scaling parameter $\beta > 0$ is used, $\psi(\rho)$ has to be replaced by $\beta^2\psi(\rho/\beta)$.

For all the radial basis functions listed in Table 1 the corresponding functions ψ can be computed analytically. The results are listed in the right column.

5.4 Boundary element discretisation

To obtain a boundary element discretisation of the problem, we approximate Γ by a conform surface triangulation with $N_{\texttt{BEM}}$ triangles and $M_{\texttt{BEM}}$ nodes. We use the piecewise constant functions (ψ_ℓ is 1 on triangle τ_ℓ and 0 outside τ_ℓ) as basis and test functions for the discretised single layer potential. These functions also serve as test functions for the

name	$\phi(\varrho)$	$\psi(\varrho)$
Gaussian	$\exp(-\varrho^2)$	$\frac{\sqrt{\pi}\,\mathrm{erf}(\varrho)}{4\varrho}$
multiquadric	$\sqrt{1+\varrho^2}$	$-\frac{-8\varrho+\varrho(5+2\varrho^2)\sqrt{1+\varrho^2}+3\,\mathrm{arcsinh}(\varrho)}{24\varrho}$
inverse quadric	$\frac{1}{1+\varrho^2}$	$-\frac{\varrho(-2+\ln(1+\varrho^2))+\arctan(\varrho)}{2\varrho}$
polyharmonic splines	$\begin{cases}\varrho^k, & k=1,3,\dots\\ \varrho^k\ln(\varrho), & k=2,4,\dots\end{cases}$	$\begin{cases}-\frac{\varrho^{k+2}}{(k+2)(k+3)}, & k=1,3,\dots\\ \frac{\varrho^{k+2}}{(k+2)(k+3)}\big(\frac{2k+5}{(k+2)(k+3)}-\ln(\varrho)\big), & k=2,4,\dots\end{cases}$
Wendland function $\phi_{3,0}$	$\big(1-\varrho\big)_+^2$	$\begin{cases}-\frac{1}{20}\varrho^4+\frac{1}{6}\varrho^3-\frac{1}{6}\varrho^2+\frac{1}{12}, & \varrho\le 1\\ \frac{1}{30\,\varrho}, & \varrho>1\end{cases}$
Wendland function $\phi_{3,1}$	$\big(1-\varrho\big)_+^4\big(4\varrho+1\big)$	$\begin{cases}-\frac{1}{14}\varrho^7+\frac{5}{14}\varrho^6-\frac{1}{6}\varrho^2+\frac{1}{14}, & \varrho\le 1\\ \frac{1}{42\,\varrho}, & \varrho>1\end{cases}$

Table 1: Some popular radial basis functions ϕ and corresponding functions ψ such that $-\Delta\psi(|x|)=\phi(|x|)$ for $x\in\mathbb{R}^3$.

double layer potential. The basis functions for the double layer potentials are chosen to be piecewise linear, i.e. $\varphi_j(x_i)=\delta_{ij}$, φ_j is linear on each τ_ℓ. Thus the BEM Galerkin procedure consists of the following steps. An initial step is a computation of the BEM matrices, namely the double layer potential matrix

$$K_h\in\mathbb{R}^{N_{\mathtt{BEM}}\times M_{\mathtt{BEM}}}\,,\quad K_h[k,j]=\frac{1}{4\pi}\int\limits_{\tau_k}\int\limits_{\Gamma}\frac{(x-y,n_y)}{|x-y|^3}\varphi_j(y)\,ds_y\,ds_x\,,$$

the single layer potential matrix

$$V_h\in\mathbb{R}^{N_{\mathtt{BEM}}\times N_{\mathtt{BEM}}}\,,\quad V_h[k,\ell]=\frac{1}{4\pi}\int\limits_{\tau_k}\int\limits_{\tau_\ell}\frac{1}{|x-y|}\,ds_y\,ds_x\,,$$

the mixed mass matrix

$$M_h\in\mathbb{R}^{N_{\mathtt{BEM}}\times M_{\mathtt{BEM}}}\,,\quad M_h[k,j]=\int\limits_{\tau_k}\int\limits_{\Gamma}\varphi_j(y)\,ds_y\,ds_x\,,$$

and the linear mass matrix

$$M_h^{(1)}\in\mathbb{R}^{M_{\mathtt{BEM}}\times M_{\mathtt{BEM}}}\,,\quad M_h^{(1)}[i,j]=\int\limits_{\Gamma}\int\limits_{\Gamma}\varphi_j(y)\varphi_i(x)\,ds_y\,ds_x\,.$$

Note that the matrices M_h and $M_h^{(1)}$ are sparse while the matrices K_h and V_h are dense and probably require an additional approximation technique.

A further preparation step is the L_2-projection of the Dirichlet boundary condition g in the space of piecewise linear functions φ_j. This is equivalent to the numerical solution of the linear system

$$M_h^{(1)}\underline{g} = \underline{b}^{(1)}\,, \quad \underline{b}_i^{(1)} = \int\limits_\Gamma g(x)\varphi_i(x)\,ds_x\,.$$

The matrix $M_h^{(1)}$ is symmetric, positive definite and well conditioned. Thus, this system can be solved with only few CGM iterations without preconditioning up to the computer accuracy.

The preparations for the RBF interpolation consist of the computation and eventually approximation of the interpolation matrix

$$R \in \mathbb{R}^{N_p \times N_p}\,, \quad R[i,j] = \phi_j(x_i)\,.$$

Then, a series of the Poisson problems

$$-\Delta u_{k+1} = f_k\,, \quad k = 0, 1, \ldots$$

has to be solved. For $k = 0$, due to $u_0 = 0$, we get $f_0 = 0$ and we have to solve the algebraic system

$$V_h\underline{t}_1 = \Big(\frac{1}{2}M_h + K_h\Big)\underline{g}\,.$$

Thus in the first step, the Neumann datum $\underline{t}_1$ coincides with the homogeneous Neumann datum $\underline{t}_{0,1}$. For $k = 1, 2, \ldots$, the right hand side f_k is given recursively by

$$\begin{aligned} f_k &= \operatorname{div}\Big(\frac{\alpha}{\alpha^*} - 1\Big)\operatorname{grad} u_k \\ &= \frac{1}{\alpha^*}(\operatorname{grad}\alpha, \operatorname{grad} u_k) + \Big(\frac{\alpha}{\alpha^*} - 1\Big)\Delta u_k \\ &= \frac{1}{\alpha^*}(\operatorname{grad}\alpha, \operatorname{grad} u_k) - \Big(\frac{\alpha}{\alpha^*} - 1\Big) f_{k-1}\,. \end{aligned}$$

There are two possibilities to compute this right hand side in all interpolation points x_j, $j = 1, 2, \ldots, N_p$. First of all, we assume that the diffusion coefficient α and, therefore, its gradient grad α are given. The gradient grad u_k can be computed by the representation formula. This is problematic in the neighbourhood of the boundary and on the boundary itself. The second possibility is to interpolate the solution u_k by the RBF's and then to use the gradient of the interpolant which is given analytically. To this end, the representation formula will be used for the points u_j inside the domain Ω and the analytically given Dirichlet boundary datum on the boundary Γ.

Thus, having the Cauchy data $\big(\underline{t}_k, g\big)$ of the function u_k, we evaluate its values $u_k(x_j)$ in all interpolation points x_j, $j = 1, 2, \ldots, N_p$, solve the interpolation system of linear equations

$$R\underline{u}_{k,N_p} = \underline{u}_k\,, \quad (\underline{u}_k)_j = u_k(x_j)$$

and obtain an easily analytically differentiable function

$$u_{k,N_p} = \sum_{j=1}^{N_p} (\underline{u}_{k,N_p})_j \phi_j \,.$$

By the use of the gradient of this function, we compute the right hand side f_k with the help of the above recursion, solve the second interpolation problem

$$R\underline{f}_{k,N_p} = \underline{f}_k \,, \quad (\underline{f}_k)_j = f_k(x_j)$$

and an approximation of the particular solution u_{p,k,N_p} reads

$$u_{p,k,N_p} = \sum_{j=1}^{N_p} (\underline{f}_{k,N_p})_j \psi_j \,.$$

Its Dirichlet trace on the boundary Γ is

$$g_{p,k,N_p} = \gamma_0 u_{p,k,N_p}$$

and its L_2-projection is obtained from the linear system

$$M_h^{(1)} \underline{g}_{p,k,N_p} = \underline{b}_{p,k,N_p} \,, \quad (\underline{b}_{p,k,N_p})_i = \int_\Gamma g_{p,k,N_p}(x) \varphi_i(x) \, ds_x \,.$$

Finally, the coefficient vector of the new homogeneous Neumann trace $\underline{t}_{0,k+1}$ fulfils

$$V_h \underline{t}_{0,k+1} = \Big(\frac{1}{2} M_h + K_h \Big) (\underline{g} - \underline{g}_{p,k,N_p})$$

and the new Cauchy data reads

$$\big(\underline{t}_{k+1}, g \big) = \big(t_{0,k+1} + \gamma_1 u_{p,k,N_p}, g \big) \,.$$

We note that all the matrices involved in this algorithm are computed in advance and decomposed or approximated in an initial step leading to a fast numerical solution of all above linear systems.

5.5 Adaptive Cross Approximation

The initial analytical form of the ACA algorithm was designed to interpolate and, hopefully, to approximate a given function K of two variables x and y by a degenerate function S_n, i.e.

$$K(x,y) \approx S_n = \sum_{\ell=1}^{n} u_\ell(x) v_\ell(y) \,. \tag{26}$$

The construction is as follows. Let X and Y be discrete point sets in $\mathbb{R}^3$.

Algorithm 1.

1. `initialisation`

   `1.1 set initial residuum and initial approximation`

$$R_0(x,y) = K(x,y)\,, \quad S_0(x,y) = 0$$

   `1.2 choose initial pivot position`

$$x_0 \in X\,, \;\; y_0 \in Y\,, \;\; R_0(x_0,y_0) \neq 0$$

2. `recursion for` $k = 0, 1, \ldots$

   `2.1 new residuum`

$$R_{k+1}(x,y) = R_k(x,y) - \frac{R_k(x,y_k)R_k(x_k,y)}{R_k(x_k,y_k)}$$

   `2.2 new approximation`

$$S_{k+1}(x,y) = S_k(x,y) + \frac{R_k(x,y_k)R_k(x_k,y)}{R_k(x_k,y_k)}$$

   `2.3 new pivot position`

$$x_{k+1} \in X\,, \;\; y_{k+1} \in Y\,, \;\; R_{k+1}(x_{k+1},y_{k+1}) \neq 0$$

After $n \geq 1$ steps of the ACA-Algorithm 1, we obtain a sequence of residua $R_0, \ldots, R_n$ and a sequence of approximations $S_0, \ldots, S_n$ with the following properties.

1. Approximation property for $k = 0, \ldots, n$

$$R_k(x,y) + S_k(x,y) = K(x,y)\,, \;\; x \in X\,, y \in Y \tag{27}$$

2. Interpolation property for $k = 1, \ldots, n$ and $\ell = 0, \ldots, k-1$

$$R_k(x,y_\ell) = R_k(x_\ell,y) = 0\,, \;\; x \in X\,, y \in Y \tag{28}$$

   or

$$S_k(x,y_\ell) = K(x,y_\ell)\,, \;\; x \in X\,, \quad S_k(x_\ell,y) = K(x_\ell,y)\,, \;\; y \in Y \tag{29}$$

3. Harmonicity property for $k = 0, \ldots, n$
   If

$$\mathcal{L}_x K(x,y) = 0\,, \;\; x \in \Omega$$

   then

$$\mathcal{L}_x R_k(x,y) = \mathcal{L}_x S_k(x,y) = 0\,, \;\; x \in \Omega$$

4. Non-recursive representation for $k = 1, \ldots, n$

$$S_k(x, y) = u_k^\top(x) V_k^{-1} w_k(y)\,,\ V_k \in \mathbb{R}^{k\times k}\,,\ u_k(x), w_k(y) \in \mathbb{R}^k \tag{30}$$

with

$$u_k(x) = \big(K(x, y_0), \ldots, K(x, y_{k-1})\big)^\top\,,$$
$$w_k(y) = \big(K(x_0, y), \ldots, K(x_{k-1}, y)\big)^\top$$

and

$$V_k = \Big(K(x_i, y_j)\Big)_{i,j=0}^{k-1}$$

Th above properties, except the last one, can be easily seen. The proof of the non-recursive representation is more technical and can be found in [2].

Algorithm 1 can be easily modified for matrices and computes their low rank approximation.

6 Numerical examples

6.1 Direct FE solution

In the next two examples, we illustrate the accuracy and convergence of the method for a series of discretisations of the unit cube

$$\Omega = (0, 1)^3$$

as well as we state a model problem for the direct and inverse formulations.

Example 2. *We consider a constant diffusion parameter*

$$\alpha(x) = 1\,,\ x \in \Omega$$

and the analytic solution

$$u(x) = -x_1(x_1 - 1)x_2(x_2 - 1)x_3(x_3 - 1)\,,\ x \in \Omega\,.$$

Thus, the Dirichlet boundary condition is homogeneous

$$g(x) = \gamma_0 u(x) = 0\,,\ x \in \Gamma$$

and the right hand side is given by

$$f(x) = 2x_2(x_2 - 1)x_3(x_3 - 1) + 2x_1(x_1 - 1)x_3(x_3 - 1) + 2x_1(x_1 - 1)x_2(x_2 - 1)$$

for $x \in \Omega$.

Table 2: Numerical results for the FEM solution, Example 1

N_1	N	L_2-Norm	CF	H^1-Norm	CF	Iter
4	27	$4.02 \cdot 10^{-4}$	-	$8.41 \cdot 10^{-4}$	-	4
8	343	$9.88 \cdot 10^{-5}$	4.06	$4.18 \cdot 10^{-4}$	2.01	16
16	3 375	$2.46 \cdot 10^{-5}$	4.02	$2.08 \cdot 10^{-4}$	2.01	29
32	29 791	$6.13 \cdot 10^{-6}$	4.01	$1.04 \cdot 10^{-4}$	2.00	65
64	250 047	$1.53 \cdot 10^{-6}$	4.01	$5.21 \cdot 10^{-4}$	2.00	130
128	2 097 152	$3.83 \cdot 10^{-7}$	3.99	$2.60 \cdot 10^{-4}$	2.00	261
256	16 581 375	$9.58 \cdot 10^{-8}$	4.00	$1.30 \cdot 10^{-4}$	2.00	548

The numerical results are presented in Table 2. The number of elements in one space dimension $N_1 = N_2 = N_3$ is listed in the first column of the table. The second column contains the number of unknowns, while in the third column of Table 2 the relative L_2-norm of the error is given. The fourth column of this table shows the convergence factor for the L_2 norm. Note that the convergence is quadratic in $h = 1/n$. The relative error in the Sobolev norm

$$\|u\|_{H^1} = \left(\int_\Omega \left(u^2 + |\operatorname{grad} u|^2 \right) dx \right)^{1/2}$$

is listed in the next column and the convergence factor in column six. The convergence is, as expected, linear. Finally in the last column, we show the number of iterations of the CG method without preconditioning for the relative accuracy $\varepsilon_{\texttt{CGM}} = 1.0 \cdot 10^{-15}$. Also its behaviour is as expected.

Example 3. *In the second example we choose*

$$\Gamma_1 = \Big\{ x \in \Gamma \,:\, x_3 = 1 \Big\}$$

and

$$g(x) = \gamma_0 u(x) = \Big(\sin(\pi\, x_1) \sin(\pi\, x_2) \Big)^2 \,,\ x \in \Gamma_1 \,.$$

We consider

$$\alpha(x) = \begin{cases} 1 + \dfrac{1}{2\, r^4} \Big(|x - x^*|^2 - r^2 \Big)^2 & \text{for} \quad |x - x^*| - r < 0 \\ 1 & \text{for} \quad |x - x^*| - r \geq 0 \end{cases} \tag{31}$$

as a diffusion coefficient, i.e. a ball like inclusion at x^* of the radius r.

The boundary condition on Γ_1 is shown in Figure 1 and the diffusion coefficient for $x^* = (0.7, 0.7, 0.7)^\top$ and $r = 0.25$ in Figure 2.

There is no analytic solution of this problem. The numerical Neumann datum shown in Figure 3 for $N_1 = N_2 = N_3 = 32$ elements in one direction or $N = 29\,791$ unknowns

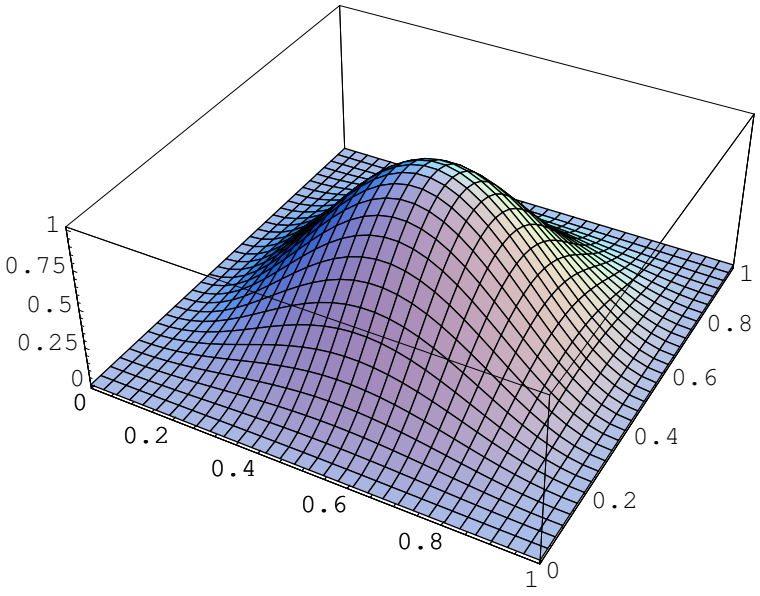

Figure 1: Boundary condition at $x_3 = 1$

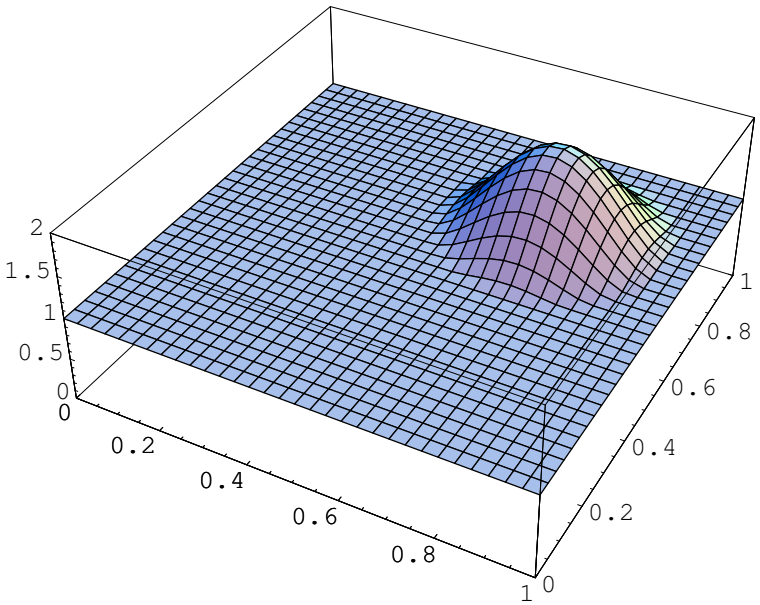

Figure 2: Diffusion coefficient at $x_3 = 0.7$

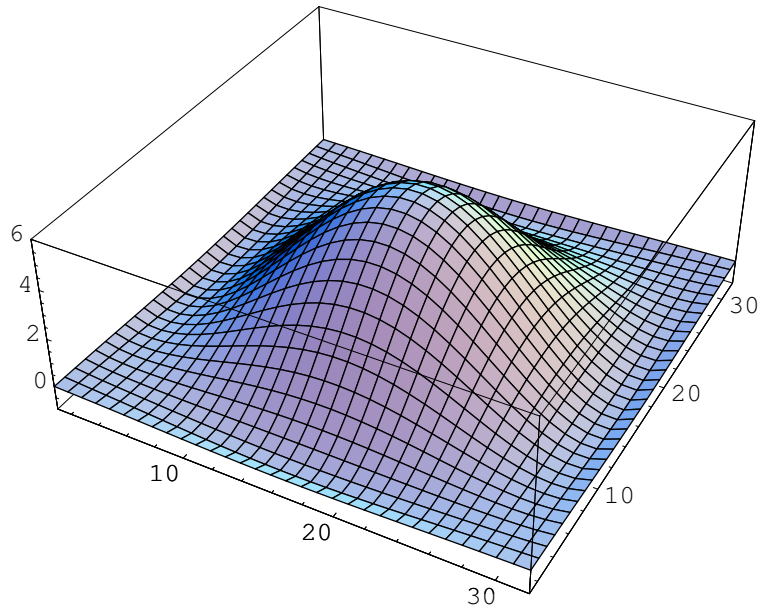

Figure 3: Neumann datum at $x_3 = 1.0$

was obtained after 153 CGM iteration for the accuracy $\varepsilon_{\texttt{CGM}} = 1.0 \cdot 10^{-15}$. In Figure 4, we show the Neumann datum obtained for the same boundary condition but for the constant diffusion coefficient $\alpha(x) = 1$. Optically, the results are very similar. However, Figure 5 shows the difference of the both solution and Figure 6 the corresponding contours. This example seems to be suitable for both, direct and inverse formulations.

6.2 Iterative FE solution

Example 4. *We consider again the diffusion coefficient (31) and the series of discretisation as in the first example.*

For the pure FEM formulation, the direct iteration (4) takes the form

$$\underline{u}_0 = 0\,, \quad A_{\alpha^*}\underline{u}_{k+1} = \Big(A_{\alpha^*} - A_\alpha\Big)\underline{u}_k + \underline{f}\,, \quad k = 0, 1, \dots\,,$$

where the FEM matrices A_{α^*} and A_α correspond to the constant and variable diffusion coefficients. In Table 3, we show the number of direct iterations of the algorithm (4) needed to reach the accuracy of $\varepsilon_{\texttt{DirInter}} = 1.0 \cdot 10^{-15}$ in the discrete L_2-norm, i.e

$$\|A_\alpha \underline{u}_k - \underline{f}\|_2$$

in column three, this number is displayed for non-optimal value of $\alpha^* = 1$ while the next column shows the number of iterations for the optimal choice of $\alpha^* = 5/4$. It is clear to see that the number of direct iterations is only weakly dependent of the discretisation and bounded from above. Furthermore, for this example, the number of iterations is rather low.

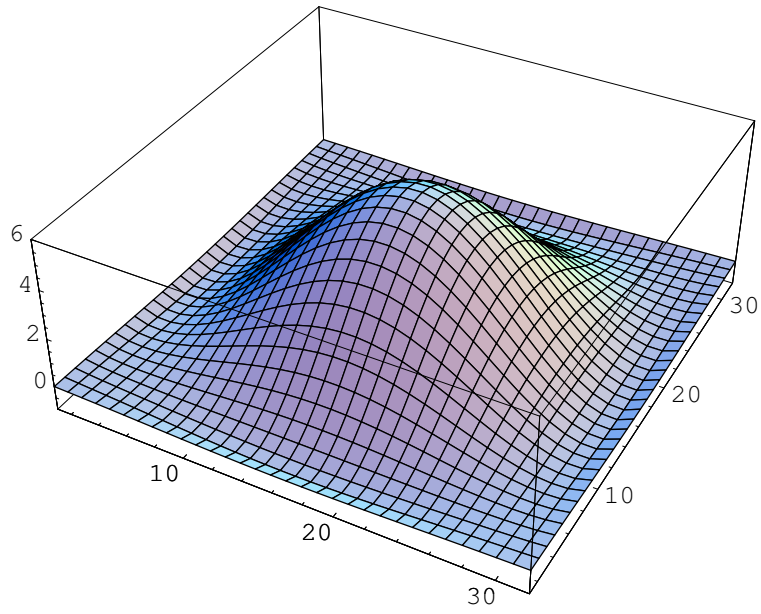

Figure 4: Initial Neumann datum at $x_3 = 1.0$

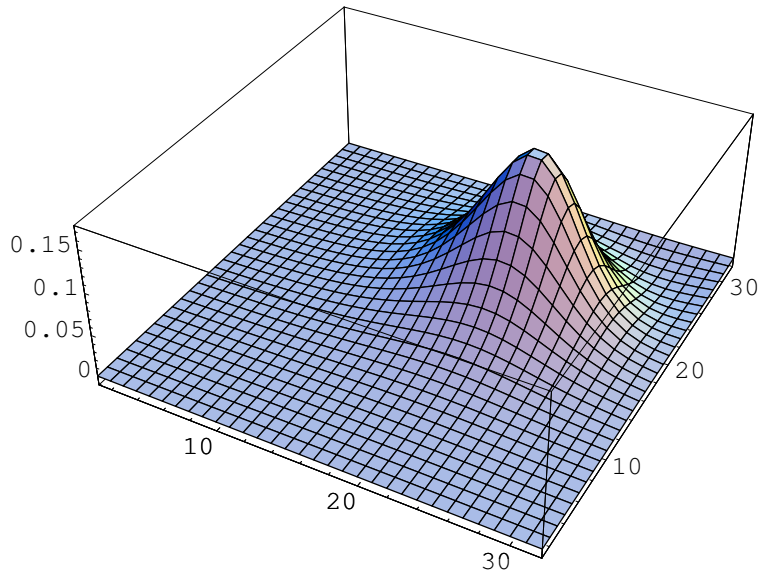

Figure 5: Difference at $x_3 = 1.0$

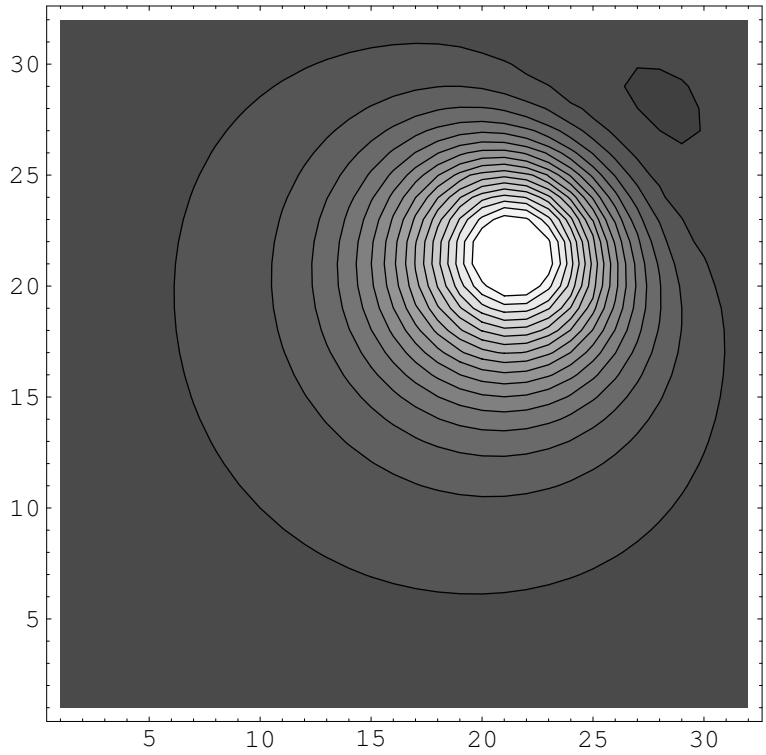

Figure 6: Contours of the difference at $x_3 = 1.0$

Table 3: Numerical results for the FEM solution, Direct iteration

N_1	N	$\alpha^* = 1$	$\alpha^* = 5/4$	CGM-Iter
4	27	17	21	7
8	343	24	21	23-25
16	3 375	31	20	48-50
32	29 791	31	19	89-120
64	250 047	29	19	175-202
128	2 097 152	26	18	347-402
256	16 581 375	23	17	686-790

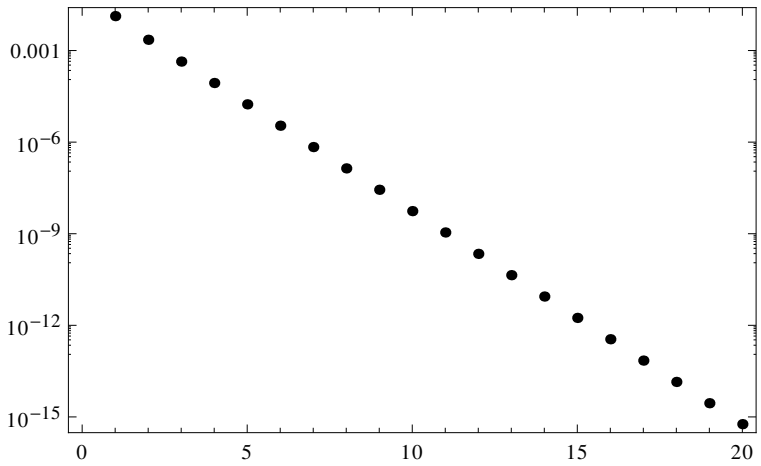

Figure 7: Convergence history for $N = 3\,375$

The last column shows the number of CGM-Iterations during each of the direct iteration which slightly varies. The CGM-accuracy was as in all above examples $\varepsilon_{\texttt{CGM}} = 1.0 \cdot 10^{-15}$. In Figure 7, we show the convergence history for $N = 3\,375$ for the optimal value $\alpha^* = 5/4$. Note that the scale of this plot is logarithmic. Figure 8 shows the convergence factor, i.e. a quotient of two consecutive errors. The theoretically predicted convergence factor $\Theta = 1/5$ can be perfectly seen in this plot.

6.3 Direct BE solution

Example 5. *We again consider a constant diffusion parameter*

$$\alpha(x) = 1\,, \;\; x \in \Omega$$

and the analytic solution

$$u(x) = \frac{1}{4\pi\,|x - x^*|}\,, \;\; x \in \Omega$$

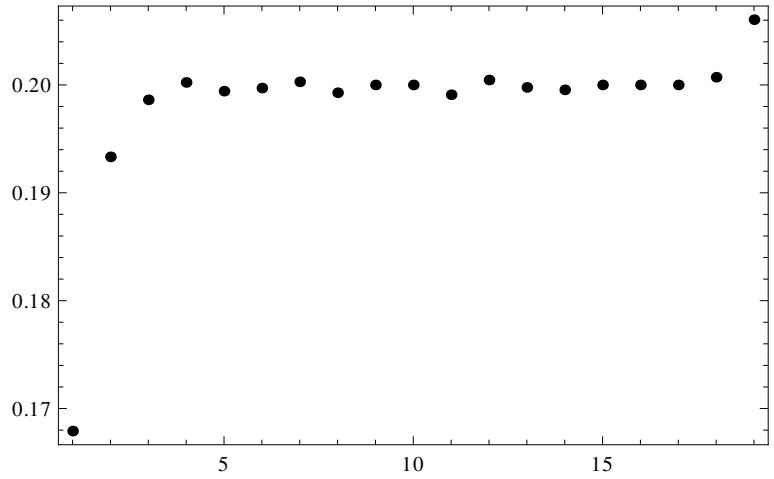

Figure 8: Convergence factor for $N = 3\,375$

Table 4: Numerical results for the BEM solution, ACA

$M_{\mathtt{BEM}}$	$N_{\mathtt{BEM}}$	$\varepsilon_{\mathtt{ACA}}$	$Mem(K_h)$	%	$Mem(V_h)$	%
386	768	$1.00 \cdot 10^{-3}$	2.00	88.46	1.67	37.05
1538	3072	$1.00 \cdot 10^{-4}$	17.36	48.15	13.35	18.54
6146	12288	$1.00 \cdot 10^{-5}$	121.95	21.17	99.16	8.61
24578	49152	$1.00 \cdot 10^{-6}$	723.74	7.85	674.34	3.66
98306	196608	$1.00 \cdot 10^{-7}$	3939.79	2.67	4230.20	1.43

for $x^* = (1.5, 1.5, 1.5)^\top$. *Thus, the function* u *is harmonic in* Ω *and its trace* $g(x) = \gamma_0 u(x)$ *will be used as the Dirichlet boundary condition in (10).*

We consider the same discretisation sequence of the unit cube as for FEM and dividing all surface rectangles in two triangles, we obtain a regular triangulation of the surface Γ. In Figure 9 an example of such discretisation for $N_{\mathtt{BEM}} = 3072$ boundary elements. The quality of the ACA approximation is illustrated in Table 4. In the first column of this table, the number $M_{\mathtt{BEM}}$ of boundary nodes is displayed while the second column shows the number of boundary elements $N_{\mathtt{BEM}}$. The required relative ACA accuracy $\varepsilon_{\mathtt{ACA}}$ is presented in third column. The fourth column contains the memory requirements data for the $N_{\mathtt{BEM}} \times M_{\mathtt{BEM}}$ double layer potential matrix K_h in Mbytes and the fifth the corresponding percentage with respect to the full memory. The same data for the $N_{\mathtt{BEM}} \times N_{\mathtt{BEM}}$ single layer potential matrix V_h is shown in columns six and seven. The increasing accuracy of the ACA approximation is necessary to guarantee the optimal order of BEM convergence which can be seen in Table 5. The L_2-norm of the error in the Dirichlet and Neumann data is displayed in the columns three and five. The corresponding convergence factors in the columns four and six. The quadratic convergence for the Dirichlet as well as linear convergence for the Neumann datum is almost perfect.

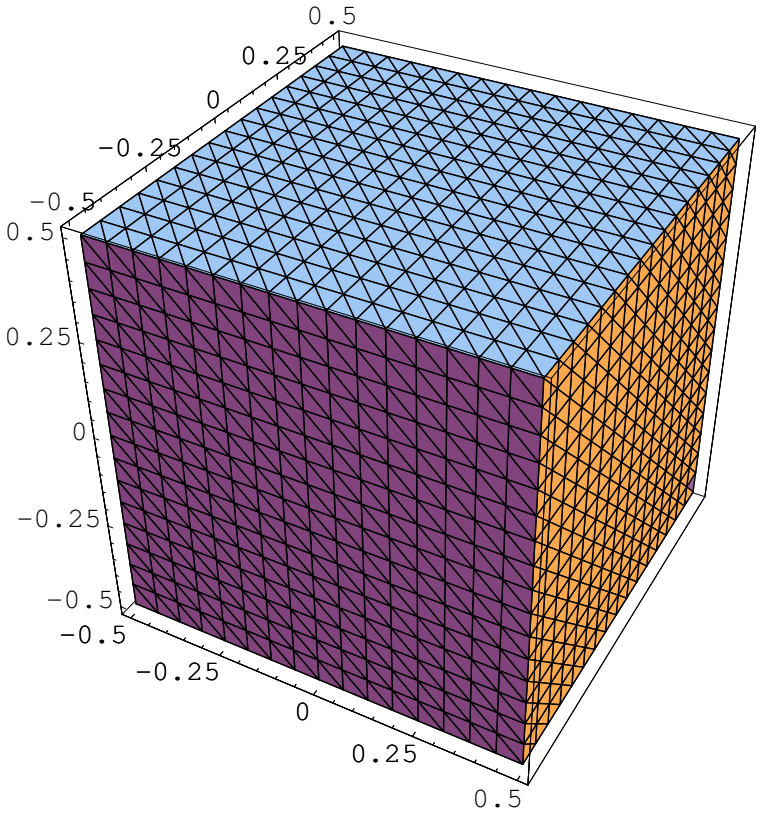

Figure 9: BEM discretisation for $N_{\texttt{BEM}} = 3072$

Table 5: Numerical results for the BEM solution, Accuracy

$M_{\texttt{BEM}}$	$N_{\texttt{BEM}}$	Dirichlet datum	CF	Neumann datum	CF
386	768	$2.01 \cdot 10^{-4}$	-	$3.32 \cdot 10^{-2}$	-
1538	3072	$4.88 \cdot 10^{-5}$	4.12	$1.57 \cdot 10^{-2}$	2.11
6146	12288	$1.20 \cdot 10^{-5}$	4.07	$7.56 \cdot 10^{-3}$	2.08
24578	49152	$2.97 \cdot 10^{-6}$	4.04	$3.71 \cdot 10^{-3}$	2.04
98306	196608	$7.39 \cdot 10^{-7}$	4.02	$1.84 \cdot 10^{-3}$	2.02

Table 6: Numerical results for the RBF interpolation, Accuracy

N_1	N_p	β	L_2	H^1	H^2
4	125	1.0	$3.36 \cdot 10^{-4}$	$3.78 \cdot 10^{-3}$	$6.60 \cdot 10^{-2}$
8	729	2.0	$2.57 \cdot 10^{-5}$	$6.19 \cdot 10^{-4}$	$2.57 \cdot 10^{-2}$
16	4913	5.0	$2.99 \cdot 10^{-6}$	$1.59 \cdot 10^{-4}$	$1.44 \cdot 10^{-2}$

6.4 RBF interpolation

Example 6. *This example illustrates the interpolation with Radial Basis Functions. We consider the infinitely smooth function defined in the unit cube* $\Omega = (0,1)^3$

$$u(x) = \frac{1}{1 + |x - x^*|^2}\,, \quad x^* = (1.5, 1.5, 1.5)^\top\,, \quad x \in \Omega\,.$$

and interpolate it in the nodes of the hexahedral FEM discretisation of Ω*. The system of interpolation functions is*

$$\phi_j(x) = \frac{1}{1 + \beta|x - x_j|^2}\,, \quad j = 1, \ldots, N_p\,,$$

where $N_p = (N_1 + 1)(N_2 + 1)(N_3 + 1)$ *is the number of nodes.*

The accuracy results are presented in Table 6. The third column of this table shows the a priori chosen parameter β of the inverse quadric function ψ while the last three columns contains the relative error of the RBF interpolation measured in the L_2 as well as in the Sobolev norms H^1 and H^2. The quality of the interpolation of the function itself and of its gradient is sufficiently high for our main task, to interpolate the right hand side of the iterative BEM solution of the direct problem.

6.5 Iterative BE solution

Here we consider the same inhomogeneous problem as in Example 3 with the diffusion coefficient (31). Again, for a non-optimal $\alpha = 1.0$ and for the optimal $\alpha^* = 1.25$, we solve a series of BEM discretisations by the use of the RBF interpolation and particular solution technique as described in Subsection 5.4. The results are shown in Table 7 where the last two columns show the number of direct iterations. Thus, the convergence results are almost the same as for the FEM discretisation. The RBF interpolation of the approximation u_k and of the right hand side f_k was performed on the $N_p = 729 = 7 \times 7 \times 7$ RBF grid independent of the BEM discretisation. We have used the norm of the difference between two subsequent approximation u_k and u_{k+1} as a stopping criteria

$$\|u_k - u_{k+1}\|_2 \leq \varepsilon_{\texttt{DirInter}}$$

with $\varepsilon_{\texttt{DirInter}} = 1.0 \cdot 10^{-15}$. The evaluation of the norm was done on the RBF interpolation grid inside the domain Ω.

Table 7: Numerical results for the FEM solution, Direct iteration

$M_{\mathtt{BEM}}$	$N_{\mathtt{BEM}}$	$\alpha^* = 1$	$\alpha^* = 5/4$
98	192	33	21
386	768	33	20
1 538	3 072	32	20
6 146	12 288	33	21

Conclusions

In this paper, we propose a new iterative procedure to solve boundary value problems with variable coefficients. We prove linear convergence with a convergence factor depending on the ratio of the maximal and the minimal value of the conductivity. This method, applied to the forward problem, can not be competitive with the standard FEM. However, it offers the possibility to apply a fast version of the Boundary Element Method based on the ACA. Numerical examples illustrate the functionality and the efficiency of the approach. The most important feature of the idea is the possibility to apply the proposed iterative procedure for the inverse problem of reconstructing the electric conductivity of a body from boundary measurements.

References

[1] H. Andrä, R. Grzibovski, and S. Rjasanow. Boundary Element Method for linear elasticity with conservative body forces. In T. Apel and O. Steinbach, editors, *Advanced Finite Element Methods and Applications*, number 66 in Lecture Notes in Applied and Computational Mechanics, pages 275–297. Springer-Verlag, Berlin-Heidelberg-NewYork, 2012.

[2] M. Bebendorf. Approximation of boundary element matrices. *Numer. Math.*, 86(4):565–589, 2000.

[3] L. Borcea. Electrical impedance tomography. *Inverse Problems*, 18(6):R99–R136, 2002.

[4] C. S. Chen, C. M. Fan, and P. H. Wen. The method of approximate particular solutions for solving elliptic problems with variable coefficients. *Int. J. Comput. Methods*, 8(3):545–559, 2011.

[5] B. Kaltenbacher, A. Neubauer, and O. Scherzer. *Iterative Regularization Methods for Nonlinear ill-posed Problems*. Radon Series on Computational and Applied Mathematics. de Gruyter, Berlin, 2008.

[6] K. Knudsen, M. Lassas, J. L. Mueller, and S. Siltanen. Regularized D-bar method for the inverse conductivity problem. *Inverse Probl. Imaging*, 3(4):599–624, 2009.

[7] W. McLean. *Strongly Elliptic Systems and Boundary Integral Equations*. Cambridge University Press, Cambridge, 2000.

[8] S. Rjasanow and O. Steinbach. *The Fast Solution of Boundary Integral Equations*. Number 12 in Springer Series in Mathematical and Analytical Technology with Applications to Engineering. Springer-Verlag, Berlin-Heidelberg-NewYork, 2007.

[9] R. Schaback and H. Wendland. Kernel techniques: from machine learning to meshless methods. *Acta Numer.*, 15:543–639, 2006.

[10] S. Siltanen, J. Mueller, and D. Isaacson. An implementation of the reconstruction algorithm of A. Nachman for the 2D inverse conductivity problem. *Inverse Problems*, 16(3):681–699, 2000.

[11] G. Uhlmann. Electrical impedance tomography and caldern's problem. *Inverse Problems*, 25(12):123011, 2009.